



Inhibition of chemotherapy resistant breast cancer stem cells by a ROR1 specific antibody

Suping Zhang^{a,b,1}, Han Zhang^{b,1}, Emanuela M. Ghia^{b,1}, Jiagia Huang^c, Liufeng Wu^a, Jianchao Zhang^a, Sharon Lam^b, Yang Lei^a, Jinsong He^d, Bing Cui^b, George F. Widhopf II^b, Jian Yu^b, Richard Schwab^b, Karen Messer^{b,e}, Wenqi Jiang^c, Barbara A. Parker^b, Dennis A. Carson^{a,b,2}, and Thomas J. Kipps^{a,b,2}

^aGuangdong Key Laboratory for Genome Stability and Human Disease Prevention, Department of Pharmacology, International Cancer Center, Shenzhen University Health Science Center, 518060 Shenzhen, China; ^bMoore's Cancer Center, University of California, San Diego, La Jolla, CA 92093; ^cState Key Laboratory of Oncology in South China, Department of Medical Oncology, Collaborative Innovation Center for Cancer Medicine, Sun Yat-sen University Cancer Center, 510060 Guangzhou, China; ^dDepartment of Breast Surgery, The Peking University Shenzhen Hospital, 518036 Shenzhen, China; and ^eDivision of Biostatistics and Bioinformatics, Department of Family Medicine and Public Health, University of California, San Diego, La Jolla, CA 92093

Contributed by Dennis A. Carson, November 9, 2018 (sent for review September 26, 2018; reviewed by Caroline Ford and Kay Huebner)

Breast cancers enduring treatment with chemotherapy may be enriched for cancer stem cells or tumor-initiating cells, which have an enhanced capacity for self-renewal, tumor initiation, and/or metastasis. Breast cancer cells that express the type I tyrosine kinaselike orphan receptor ROR1 also may have such features. Here we find that the expression of ROR1 increased in breast cancer cells following treatment with chemotherapy, which also enhanced expression of genes induced by the activation of Rho-GTPases, Hippo-YAP/TAZ, or B lymphoma Mo-MLV insertion region 1 homolog (BMI1). Expression of ROR1 also enhanced the capacity of breast cancer cells to invade Matrigel, form spheroids, engraft in Rag2^{-/-}γc^{-/-} mice, or survive treatment with paclitaxel. Treatment of mice bearing breast cancer patient-derived xenografts (PDXs) with the humanized anti-ROR1 monoclonal antibody cirmtuzumab repressed expression of genes associated with breast cancer stemness, reduced activation of Rho-GTPases, Hippo-YAP/TAZ, or BMI1, and impaired the capacity of breast cancer PDXs to metastasize or reengraft Rag2^{-/-}γc^{-/-} mice. Finally, treatment of PDX-bearing mice with cirmtuzumab and paclitaxel was more effective than treatment with either alone in eradicating breast cancer PDXs. These results indicate that targeting ROR1 may improve the response to chemotherapy of patients with breast cancer.

breast-cancer stem cells | chemotherapy | ROR1 | ROR1-signaling | cirmtuzumab

Breast cancers enduring chemotherapy may be enriched for cells with mesenchymal or stemness features, which can enable metastases or tumor relapse (1, 2). Epithelial cancer cells that possess or acquire a mesenchymal phenotype have an enhanced capacity for migration and invasion, a process known as epithelial-to-mesenchymal transition (EMT). In addition, EMT-master-transcription factors (e.g., SNAI1) can enhance the tumor-initiation capacity of cancer cells (3, 4). Cancer cells with the capacity to regrow the tumor are called tumor-initiation cells or cancer stem cells (CSCs); such cells have the capacity to self-renew and/or differentiate and thereby repopulate the primary tumor or establish metastatic tumors at distant sites (5). Recent studies demonstrate that cancer cells may acquire stemness features of CSCs in response to signals derived from the tumor microenvironment and/or following treatment with chemotherapy (5). If so, then targeting the CSC pathways that induce EMT and/or that account for the acquisition of tumor stemness may be more effective than strategies that only target existent CSCs (6). CSCs with stemness features have the distinctive capacity to form nonadherent cellular spheroids or engraft immune-deficient mice (1, 7). Such cells have gene-expression signatures that reflect their relatively high capacity for self-renewal and ability to regenerate the entire tumor population (1). Notable is the expression of B lymphoma Mo-MLV insertion region 1 homolog (BMI1), a transcription repressor that belongs to the polycomb-group family of proteins; high-level expression of BMI1 is associ-

ated with breast cancers that have a basal-like phenotype, which typically is associated with relatively poor survival (8). BMI1 promotes self-renewal and the acquisition of a tumor-initiation capacity associated with CSCs (9–13). Moreover, BMI1 can promote expression of genes encoding ATP-binding cassette transporters, which can enhance resistance to chemotherapy (3, 11).

Associated with cancer stemness is ROR1 (14), a type I tyrosine kinaselike orphan receptor, which is expressed by many cancers but not by normal postpartum tissues (15, 16). Prior studies found that breast cancers with high levels of ROR1 typically were poorly differentiated and expressed markers associated with EMT (15, 17). High-level breast cancer-cell expression of ROR1 associates with a relatively rapid relapse after therapy and short survival (15, 17, 18). On the other hand, silencing *ROR1* could repress the expression of genes associated with EMT and/or impair cancer-cell migration/invasion and metastasis, indicating that ROR1 may play a role in inducing stemness of breast cancer cells (17).

ROR1 can serve as a receptor for Wnt5a (19), which may be expressed by tumor cells or by accessory cells within tumor microenvironment (20, 21). Wnt5a can induce noncanonical Wnt signaling in chronic lymphocytic leukemia (CLL), leading to activation of Rho-GTPases and enhanced tumor-cell migration,

Significance

We report that breast cancer cells surviving treatment with paclitaxel express relatively high levels of ROR1, which can induce activation of stem-cell signaling pathways in response to Wnt5a. A humanized anti-ROR1 drug, cirmtuzumab, can inhibit ROR1-dependent activation of such signaling and impair the capacity of post-treatment breast cancer cells to metastasize or reengraft immune-deficient mice.

Author contributions: S.Z., H.Z., E.M.G., B.A.P., and T.J.K. designed research; S.Z., H.Z., L.W., J.Z., S.L., Y.L., B.C., and J.Y. performed research; J. Huang, J. He, G.F.W., R.S., and W.J. contributed new reagents/analytic tools; S.Z., H.Z., E.M.G., L.W., J.Z., K.M., and T.J.K. analyzed data; and S.Z., H.Z., E.M.G., B.A.P., D.A.C., and T.J.K. wrote the paper.

Reviewers: C.F., University of New South Wales; and K.H., Ohio State University Comprehensive Cancer Center.

Conflict of interest statement: Cirmtuzumab was developed by T.J.K. in the T.J.K. laboratory and licensed by the University of California to Onternal Therapeutics, Inc., which provided stock options and research funding to the T.K.J. laboratory.

This open access article is distributed under [Creative Commons Attribution-NonCommercial-NoDerivatives License 4.0 \(CC BY-NC-ND\)](https://creativecommons.org/licenses/by-nc-nd/4.0/).

Data deposition: Raw sequencing files have been deposited in the Gene Expression Omnibus (GEO) database, <https://www.ncbi.nlm.nih.gov/geo> (accession no. [GSE108632](https://www.ncbi.nlm.nih.gov/geo/acc/show/GSE108632)).

¹S.Z., H.Z., and E.M.G. contributed equally to this work.

²To whom correspondence may be addressed. Email: dcarson@ucsd.edu or tkipps@ucsd.edu.

This article contains supporting information online at www.pnas.org/lookup/suppl/doi:10.1073/pnas.1816262116/-DCSupplemental.

Published online January 8, 2019.

of both CD44 and CD24 (CD44⁺/CD24⁺ cells) (*SI Appendix, Fig. S1 B–D*).

In tissue cultures, the PDX cells that had expressed high levels of ROR1 had a greater capacity to form spheroids than PDX cells of the same tumor that had low-to-undetectable ROR1 (*SI Appendix, Fig. S1 E–G*). Furthermore, the tumor cells of each PDX that had high-level ROR1 were more invasive in Matrigel than tumor cells of the same PDX with low-to-undetectable ROR1 (*SI Appendix, Fig. S1H*).

We implanted equal numbers of tumor cells from each PDX into Rag2^{-/-}γc^{-/-} mice and monitored the growth of secondary tumors. When these secondary tumors reached ~300 mm³ in size, we treated the mice with paclitaxel at 13.4 mg/kg per day for five consecutive days (Fig. 1*B*). The tumors derived from the PDX with high proportions of ROR1⁺ cells (e.g., PDX4 or PDX5) regrew shortly after therapy, in contrast to the tumors of mice engrafted with the PDX that had few ROR1⁺ cells (e.g., PDX1 or PDX2, Fig. 1*B*).

We excised the tumors from mice bearing PDX4 or PDX5 and examined the human breast cancer cells for the expression of ROR1. We found the breast cancer PDXs excised from paclitaxel-treated mice expressed higher levels of ROR1 than the PDXs derived from the same tumor but excised from mice that did not receive paclitaxel or the original PDXs (Fig. 1*C*). As noted in prior studies (31), the tumors of mice treated with paclitaxel also had higher proportions of ALDH1⁺ cells than the matched tumors of untreated mice or the original PDX (*SI Appendix, Fig. S1I*). Finally, the PDX cells excised from mice treated with paclitaxel had a greater capacity to form spheroids, invade Matrigel, or reengraft Rag2^{-/-}γc^{-/-} mice than the PDXs derived from the same tumor but excised from mice that did not receive treatment or the original PDX (Fig. 1*D–F*).

We isolated breast cancer cells that had high levels of ROR1 (ROR1^{Hi}) or low levels of ROR1 (ROR1^{Low}) from PDX3, PDX4, or PDX5 via flow cytometry using 4A5 (*SI Appendix, Fig. S2A*), a mAb that binds an epitope of ROR1 that is distinct from that bound by cirmtuzumab. ROR1^{Hi} cells formed significantly greater numbers of spheroids than ROR1^{Low} cells, which formed few spheroids or none at all (*SI Appendix, Fig. S2B*). Furthermore, ROR1^{Hi} cells were significantly more invasive in Matrigel than ROR1^{Low} cancer cells of the same tumor (*SI Appendix, Fig. S2C*).

We performed tumorigenicity assays with limiting numbers of tumor cells from PDX3, PDX4, or PDX5. Five hundred ROR1^{Hi} cells from each PDX could establish secondary PDXs in most mice (*SI Appendix, Fig. S2D*). In contrast, the same numbers of ROR1^{Low} cells did not form tumors except in a few animals (*SI Appendix, Fig. S2D*). Similarly, ALDH1⁺ or CD44⁺/CD24^{Low} cells isolated from these PDXs also had a significantly greater capacity to form secondary PDXs than ALDH1^{Neg} or CD44⁺/CD24⁺ cells of the same PDX (*SI Appendix, Table S3*), in agreement with prior studies (1, 7, 30).

Expression of ROR1 Associates with Activation of Hippo-YAP/TAZ and BMI1. We interrogated the PubMed Gene Expression Omnibus (GEO) database (accession no. GSE87455) on HER2-negative breast tumor biopsies obtained from patients before or after treatment with four cycles of epirubicin plus docetaxel and bevacizumab (2). Forty-three (76%) of the 57 post-treatment biopsy specimens had higher levels of *ROR1* than the matched pretreatment tumor specimens. Similarly, 48 (84%) of the matched tumor specimens had higher levels of *ALDH1A1* after therapy (*SI Appendix, Fig. S3A*). However, we did not observe a significant difference in the levels of *WNT5A* between pre- and post-treatment tumor samples (*SI Appendix, Fig. S2A*). Gene set enrichment (GSE) analysis revealed that post-treatment breast cancer cells had higher-level expression of genes associated with the activation of Rho-GTPases, Hippo-YAP/TAZ, or BMI1 than matched pretreatment tumor specimens (*SI Appendix, Fig. S3B*).

Compared with matched pretreatment breast cancer-biopsy specimens, the breast cancer tissue obtained from patients after chemotherapy expressed higher levels of genes associated with EMT, CD44⁺/CD24^{Low} CSCs, or mammosphere- (MS-) forming cells (*SI Appendix, Fig. S3B*).

We segregated the pretreatment specimens ($n = 122$) of GSE87455 into two subgroups based upon their relative expression of *ROR1*. Samples with *ROR1* levels greater than the median level expressed in all samples were designated as ROR1^{Hi} ($n = 61$), whereas tumor samples with lower *ROR1* were designated as ROR1^{Low}. The differences in gene expression between matched post- and pretreatment specimens resembled those of ROR1^{Hi} versus ROR1^{Low} breast cancers.

Of the 34,694 genes analyzed, we identified the 1,000 most overexpressed and the 1,000 most underexpressed genes differentially expressed in post-treatment versus pretreatment breast cancer specimens or in ROR1^{Hi} versus ROR1^{Low} breast cancers. Three-hundred-sixty-five of the 1,000 most overexpressed transcripts after chemotherapy were among the 1,000 most overexpressed in ROR1^{Hi} cancers relative to ROR1^{Low} breast cancers (e.g., *ALDH1A1*); only three of these 1,000 genes were among the 1,000 most overexpressed in ROR1^{Low} tumors relative to ROR1^{Hi} tumors ($P < 0.0001$, Fisher's exact test). Conversely, 190 of the 1,000 most underrepresented transcripts after chemotherapy were among the 1,000 most under-represented in ROR1^{Hi} breast cancers relative to ROR1^{Low} breast cancers; none of the 1,000 most under-represented genes after chemotherapy were under-represented in ROR1^{Low} tumors relative to ROR1^{Hi} cancers ($P < 0.0001$, Fisher's exact test). GSE analysis revealed that, relative to ROR1^{Low} tumors, ROR1^{Hi} tumors expressed higher levels of genes associated with the activation of Rho-GTPases (32, 33), Hippo-YAP/TAZ (34), BMI1 (35), or EMT (36) (*SI Appendix, Fig. S3C*). Similar findings were observed for samples described in the GSE21974 dataset (*SI Appendix, Fig. S3 D and E*).

Moreover, compared with ROR1^{Low} tumors, ROR1^{Hi} breast cancers also had higher expression of genes that were distinctively overexpressed in embryonic stem cells, including those activated by Oct4 or overlapping targets of Nanog, Oct4, and Sox2 (*SI Appendix, Table S4*) (37). Finally, ROR1^{Hi} breast cancers expressed higher levels of genes that distinctively were overexpressed by CD44⁺/CD24^{Low} CSCs or MS-forming cells relative to CD44⁺/CD24⁺ non-CSCs or all tumor cells (1). Collectively, these analyses indicate that therapy induced changes in gene expression that more resembled those distinguishing ROR1^{Hi} from ROR1^{Low} breast cancers, potentially reflecting treatment-related increases in the proportions of ROR1⁺ cells and/or increased expression of genes induced by ROR1 signaling rather than a direct effect of chemotherapy per se.

Wnt5a Induces ROR1-Dependent Activation of Rho-GTPases, YAP/TAZ, and BMI1. We extinguished *ROR1* via CRISPR/Cas9 in the basal-type breast cancer cell-line Hs578T (Fig. 2*A*). Exogenous Wnt5a could induce activation of Rac1, RhoA, and cdc42 within 10 min in wild-type Hs578T cells (wt-Hs578T) but not in ROR1^{-/-} Hs578T cells lacking ROR1 (ROR1^{-/-} Hs578T) (Fig. 2*A*). Treatment with Wnt5a also enhanced expression and nuclear localization of YAP/TAZ in wt-Hs578T cells but not in ROR1^{-/-} Hs578T (Fig. 2*B and C*).

Moreover, treatment with exogenous Wnt5a for 2 h enhanced expression of BMI1 protein but not *BMI1* messenger RNA in wt-Hs578T cells but not ROR1^{-/-} Hs578T cells (Fig. 2*D and SI Appendix, Fig. S4A*), suggesting that Wnt5a induced increases in BMI1 by interfering with its degradation.

We examined whether Wnt5a could induce Hs578T cells to activate AKT, which prior studies found could inhibit proteasomal degradation and promote accumulation of BMI1 (38). Wnt5a induced AKT phosphorylation in wt-Hs578T cells but not in ROR1^{-/-}

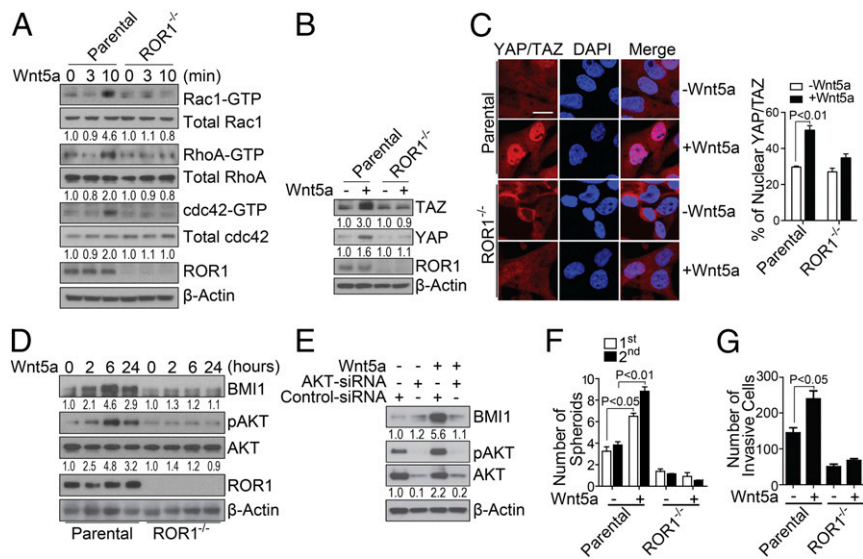


Fig. 2. Wnt5a induces ROR1-dependent activation of Rho-GTPases, YAP/TAZ, and BMI1. (A) Immunoblot analyses for proteins as indicated on the right using lysates prepared from Hs578T cells (Parental) or Hs578T knocked out for ROR1 ($ROR1^{-/-}$) that were stimulated with Wnt5a for the times indicated. The numbers below each lane are the ratios of the band densities of activated versus total GTPase, normalized with respect to cells treated without Wnt5a. (B) Immunoblot analyses for proteins indicated on the right using lysates of parental or $ROR1^{-/-}$ Hs578T that were treated without (-) or with (+) Wnt5a as indicated. The numbers below each lane represent the ratios of the band densities for each protein relative to that of β -actin, normalized with respect to cells treated without Wnt5a. (C) Photomicrographs of parental (Top row) or $ROR1^{-/-}$ Hs578T cells (Bottom row) that were treated without or with Wnt5a as indicated and then stained for YAP/TAZ and 4',6-diamidino-2-phenylindole (DAPI) as indicated and then examined using confocal microscopy. (Scale bar: 20 μ m.) The histogram to the Right of the photomicrographs provides the average percentages of YAP/TAZ located within the nuclei of the cells in each field ($n = 10$, \pm SEM). (D) Immunoblot analyses for proteins indicated on the right using lysates of parental or $ROR1^{-/-}$ Hs578T (as indicated on the Bottom) that were treated with Wnt5a for the times indicated. The numbers below each lane are the ratios of band densities of BMI1 versus β -actin or pAKT versus total AKT normalized to that of the sample collected at time 0. (E) Immunoblot analyses for proteins indicated on the right using lysates of Hs578T that had been treated with control small interfering RNA (siRNA) or AKT-specific siRNA (AKT-siRNA) as indicated. The numbers below each lane are as in Fig. 3D. (F and G) The histograms depict the average numbers of spheroids (F) or invasive cells (G) from parental or $ROR1^{-/-}$ Hs578T that were treated without or with Wnt5a in triplicate \pm SEM.

Hs578T cells (Fig. 2D). On the other hand, treatment of wt-Hs578T with siRNA specific for AKT or a small molecule inhibitor of AKT (MK-2206) impaired the capacity of Wnt5a to induce activation of AKT and inhibited the capacity of Wnt5a to enhance expression of BMI1 (Fig. 2E and *SI Appendix*, Fig. S4B). Functionally, $ROR1^{-/-}$ Hs578T cells formed significantly fewer spheroids than wt-Hs578T cells (Fig. 2F). Also, treatment with exogenous Wnt5a enhanced the capacity of wt-Hs578T cells but not $ROR1^{-/-}$ Hs578T to invade Matrigel (Fig. 2G).

Cirmtuzumab Inhibits Wnt5a-Induced Activation of Rho-GTPases, Hippo-YAP/TAZ, and BMI1 in Breast Cancer. We examined whether cirmtuzumab could inhibit Wnt5a-induced activation of Rho-GTPases, Hippo-YAP/TAZ, or BMI1. Treatment of wt-Hs578T cells with cirmtuzumab but not a human immunoglobulin G (hIgG) of irrelevant specificity, inhibited the capacity of exogenous Wnt5a to induce activation of Rac1, RhoA, or cdc42 (Fig. 3A), nuclear localization of TAZ (Fig. 3B and C), activation of AKT, or expression of BMI1 (Fig. 3D and E). Furthermore, treatment with cirmtuzumab but not control hIgG could block Wnt5a from enhancing the capacity of wt-Hs578T to form spheroids (Fig. 3F) or invade Matrigel (Fig. 3G). Similarly, we found that breast cancer PDX cells, which express Wnt5a (*SI Appendix*, Fig. S5A), had significantly less nuclear TAZ after treatment for 4 h with cirmtuzumab than the same breast cancer cells treated with control hIgG (*SI Appendix*, Fig. S5B). Moreover, cirmtuzumab but not control hIgG could reduce the expression of BMI1 in breast cancer PDX cells within 6 h (*SI Appendix*, Fig. S5C) and inhibit the capacity of these cells to form spheroids or invade Matrigel (*SI Appendix*, Fig. S5D and E).

Cirmtuzumab Inhibits Reengraftment of Breast Cancer PDXs. We evaluated the activity of cirmtuzumab on breast cancer PDXs in vivo and found that biweekly intravenous infusions of cirmtuzumab (at 10 mg/kg) significantly suppressed the development and growth of PDX tumors, including PDX3, which had low-level expression of ROR1 (Fig. 4A and *SI Appendix*, Figs. S1E and S5F and G). Moreover, treatment of mice bearing breast cancer PDXs with cirmtuzumab inhibited the development of pulmonary metastases, significantly reducing the numbers of metastatic foci from those noted in control hIgG-treated mice (Fig. 4B).

We examined the transcriptomes of breast cancer PDXs excised from cirmtuzumab-treated mice ($n = 4$) versus control-hIgG-treated mice ($n = 4$) and performed GSE analysis on the RNA-seq data (GSE108632). Tumor cells isolated from breast cancer PDXs of cirmtuzumab-treated mice expressed significantly lower levels of genes associated with the activation of Rho-GTPases, Hippo-YAP, BMI1, or EMT than cancer cells of the same PDXs isolated from control-hIgG-treated mice (Fig. 4C and *SI Appendix*, Fig. S5H). Moreover, tumors of cirmtuzumab-treated mice also expressed significantly lower levels of genes overexpressed by $CD44^{+}/CD24^{Low}$ CSC or MS-forming cells (Fig. 4C) than did matched tumors of control-hIgG-treated mice. The PDXs of cirmtuzumab-treated mice also had lower levels of ROR1, activated Rho-GTPases, YAP/TAZ, or BMI1 than matched PDXs excised from control-treated mice as assessed by immunoblot analyses (Fig. 4D).

We examined PDX cells from control-treated or cirmtuzumab-treated mice for their capacity to form secondary PDXs in $Rag2^{-/-}\gamma c^{-/-}$ mice. PDX cells isolated from cirmtuzumab-treated mice were significantly less effective in forming secondary PDXs

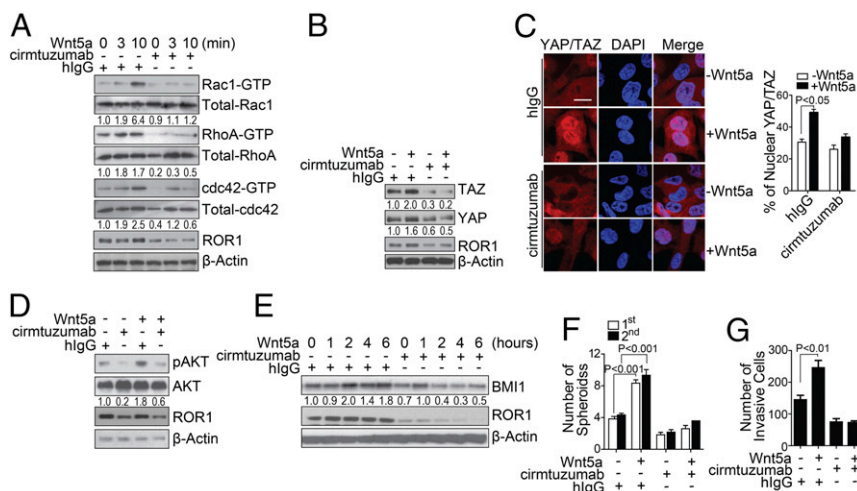


Fig. 3. Cirmtuzumab inhibits Wnt5a-induced ROR1-dependent activation of Rho-GTPases, YAP/TAZ, and BMI1. (A) Immunoblot analyses for proteins indicated on the right using lysates of Hs578T that had been treated with a control hlgG or cirmtuzumab and then stimulated with Wnt5a for the times indicated. The numbers below each lane are the ratios of the band densities of activated versus total GTPase, normalized with respect to the hlgG-treated cells without Wnt5a. (B) Immunoblot analyses for proteins indicated on the right using lysates prepared from Hs578T cultured with cirmtuzumab or hlgG and then treated without or with Wnt5a as indicated. The numbers below each lane represent the ratios of the band densities for each protein relative to that of β -actin, normalized with respect to the hlgG-treated cells without Wnt5a. (C) Photomicrographs of Hs578T cultured overnight with cirmtuzumab or hlgG (as indicated on the *Left*), then treated without or with Wnt5a for 4 h (as indicated), then stained for YAP/TAZ and DAPI (as indicated), and then examined via confocal microscopy. (Scale bar: 20 μ m.) The histogram to the *Right* of the photomicrographs provides the average percentages of YAP/TAZ located within the nuclei of the cells in each field ($n = 10$, \pm SEM). (D) Immunoblot analyses for proteins indicated on the right using lysates of Hs578T that had been treated overnight with hlgG or cirmtuzumab and then treated without or with Wnt5a as indicated. The numbers below each lane are the ratios of band densities of pAKT versus total AKT, normalized with respect to the hlgG-treated cells without Wnt5a. (E) Immunoblot analyses for proteins indicated on the right using lysates of Hs578T that had been treated overnight with hlgG or cirmtuzumab and then treated with Wnt5a for the times indicated. The numbers below each lane are the ratios of band densities of BMI1 versus β -actin, normalized with respect to the hlgG-treated cells without Wnt5a. (F and G) The bar graph depicts the average numbers of spheroids (F) or invasive cells (G) from Hs578T cells that were incubated with hlgG or cirmtuzumab overnight and then treated with or without Wnt5a in three separate culture wells \pm SEM. The open bars indicate the number of spheroids detected during the first passage, whereas the closed bars provide those of the second passage in three separate culture wells \pm SEM.

than tumor cells of the same PDXs isolated from mice treated with hlgG (Fig. 4E). Collectively, these data indicate that treatment with cirmtuzumab inhibited the stemness of breast cancer cells *in vivo*.

Treatment with Paclitaxel and Cirmtuzumab Achieves Greater Tumor Clearance than Treatment with Either Alone. We treated PDX4- or PDX5-bearing mice with cirmtuzumab (10 mg/kg), paclitaxel (13.4 mg/kg) (39), or the combination of cirmtuzumab and paclitaxel. Treatment with cirmtuzumab and paclitaxel was significantly more effective in reducing tumor volumes than treatment with either cirmtuzumab or paclitaxel alone (Fig. 5A), each of which significantly inhibited tumor growth relative to that of control-treated animals. The tumor cells isolated from the PDXs of mice treated with cirmtuzumab and paclitaxel had lower levels of ROR1, activated Rho-GTPases, phosphorylated AKT, YAP/TAZ, and BMI1 than did the tumor cells of the same PDXs excised from mice treated with paclitaxel alone (Fig. 5B). These data demonstrate that the combination of cirmtuzumab and paclitaxel had complementary antitumor activity.

We isolated tumor cells of PDXs that recurred in animals after therapy and studied their relative capacity to form secondary PDXs when engrafted in other immune-deficient mice. We found that the tumor cells of the PDXs from mice treated with single-agent paclitaxel readily developed secondary PDXs. However, the tumor cells isolated from cirmtuzumab-treated mice were significantly less effective in generating secondary PDXs than the tumor cells isolated from animals treated with paclitaxel or hlgG. However, none of the mice engrafted with tumor cells isolated from mice treated with cirmtuzumab and paclitaxel developed detectable tumors (Fig. 5C).

Discussion

Tumor recurrence following treatment with chemotherapy may develop from chemotherapy-resistant preexisting CSCs or from enduring cancer cells that subsequently acquire self-renewing and/or tumor-initiating capacities, resulting from chemotherapy-induced changes in the tumor or its microenvironment (niche signaling) (40, 41). Here, we report that breast cancer cells surviving chemotherapy expressed higher levels of ROR1, which was associated with the activation of pathways induced by ROR1 signaling (e.g., Hippo-YAP/TAZ and BMI1). Blocking ROR1 signaling with the humanized anti-ROR1 mAb cirmtuzumab diminished the activation of such pathways, the development of metastases, or the capacity of cancer cells to persist after chemotherapy.

ROR1 signaling may contribute to the maintenance, self-renewal, and drug resistance of cancer cells. Consistent with this notion, we found that expression of genes associated with the activation of Rho-GTPases was increased in breast cancer cells with high levels of ROR1. Prior studies found that Rho-GTPase signaling is altered in human breast tumors, and the elevated expression and activation of Rho-GTPases correlates with tumor progression, metastasis, and poor prognosis (23, 42). Furthermore, the activation of Rac1 may promote the survival of breast cancer cells during radiation therapy (24).

High-level expression of ROR1 in primary breast cancer also was associated with high levels of BMI1. Wnt5a/ROR1 signaling may enhance the expression of BMI1 through its capacity to activate AKT, which can phosphorylate BMI1 at three highly conserved serine residues thereby reducing the rate of BMI1 protein degradation (43). The resulting increase in BMI1 may account, in part, for the enhanced capacity of ROR1^{Hi} breast cancer cells to initiate tumor growth, spread to distal sites, or resist the cytotoxic effects of chemotherapy relative to breast cancer cells lacking

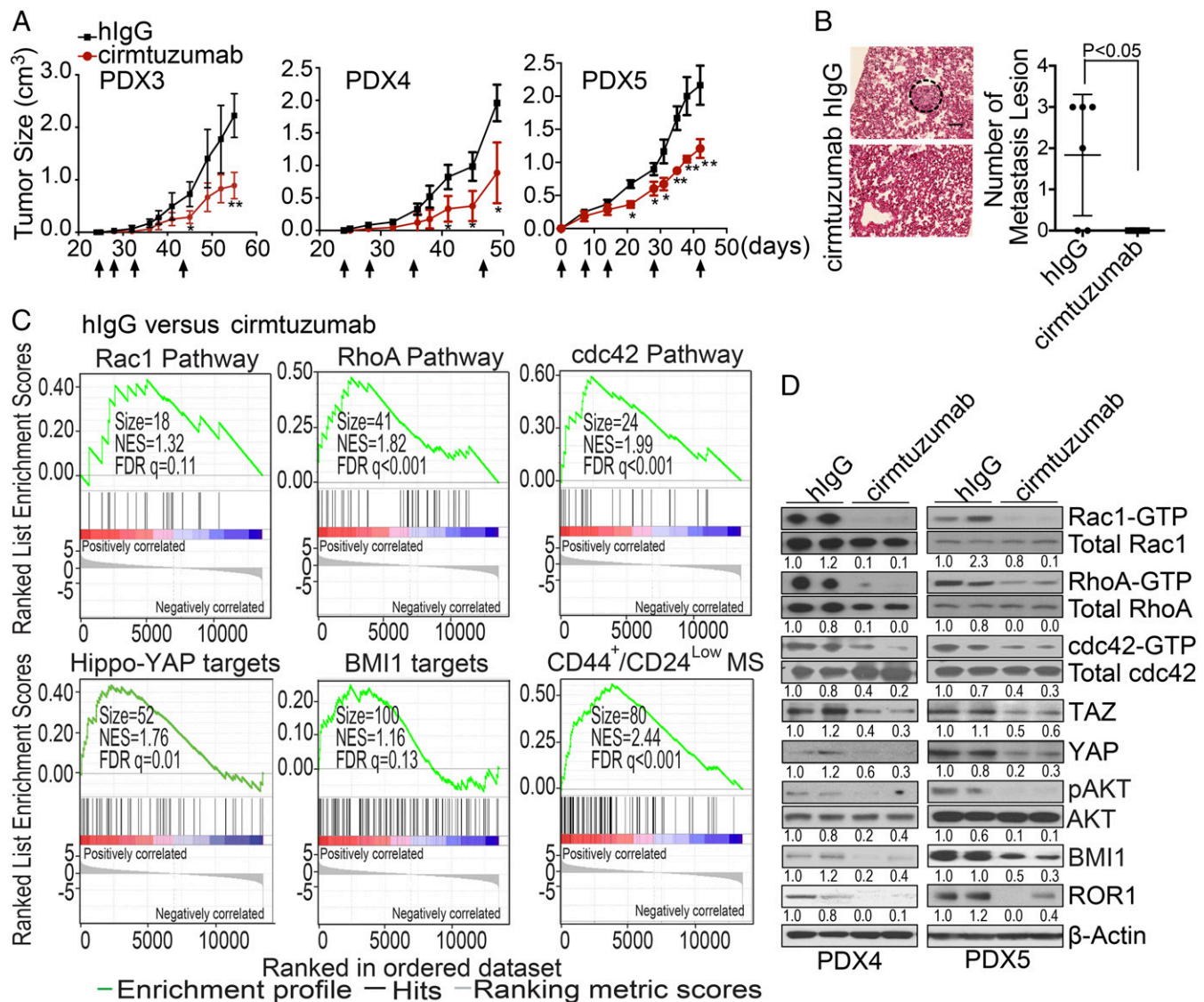


Fig. 4. Cirmtuzumab inhibits stemness of breast cancer PDXs. (A) The line graph depicts the mean tumor growth of each of PDX3, PDX4, and PDX5 over time (\pm SEM, $n = 6-8$) for animals that did not receive treatment (black line) or that were treated with cirmtuzumab (red line) on the days indicated by the black arrows. One asterisk indicates $P < 0.05$, and two asterisks indicate $P < 0.01$ using Student's t Test. (B) Hematoxylin and eosin staining of lung tissue from a representative tumor-bearing mouse engrafted with cells of PDX5 and treated with control hlgG or cirmtuzumab as indicated. A dashed-lined circle highlights metastatic foci. (Scale bar: 100 μ m.) The scatter plot shows the average numbers of metastatic foci that were found in the lungs of each animal by the treatment group (\pm SEM, $n = 6$). (C) Enrichment plots of genes associated with the activation of Rho-GTPases, Hippo-YAP, BMI1, or gene signature common on both CD44⁺/CD24^{Low} cancer stem cells and MS-forming cells in PDXs derived from PDX4 in mice treated with control hlgG versus cirmtuzumab as assessed via RNA sequencing (RNA-seq) (GSE108632). (D) Immunoblot analyses for proteins indicated on the right using lysates prepared from PDX4 or PDX5 (as indicated on the *Bottom*) that were extirpated from mice treated with control hlgG or cirmtuzumab as indicated. The numbers below each row are the ratios of band densities of activated versus total GTPase, pAKT versus total AKT, BMI1, TAZ/YAP versus β -actin, or ROR1 versus β -actin, normalized to that of the first control sample. (E) Table providing the numbers of mice that developed tumors (numerator) versus the numbers of mice implanted (denominator) with cells from PDX3, PDX4, or PDX5 (as indicated in the left column), which were removed from mice treated with either hlgG or cirmtuzumab (as indicated in the second column). For these experiments, mice were given varying numbers of tumor cells (as indicated in the row below "cell number"). The frequencies of tumorigenic cells computed using ELDA software are provided in the penultimate right column. The P values indicate the significance of the difference between the tumorigenic frequencies of tumor cells recovered from hlgG- versus cirmtuzumab-treated mice.

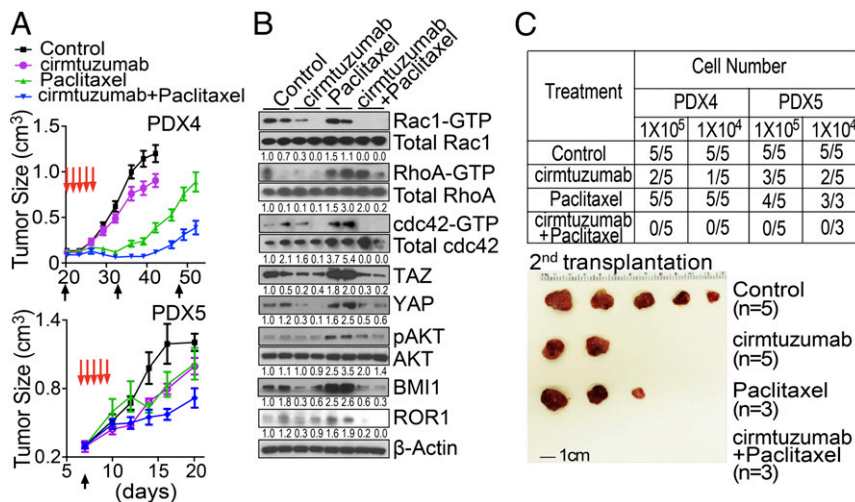


Fig. 5. Cirmtuzumab and paclitaxel have complementary antitumor activity. (A) The line graph depicts the mean tumor growth of PDX4 or PDX5 over time (\pm SEM, $n = 8-10$) in mice that were untreated (Control, black line) or treated with cirmtuzumab (purple line), paclitaxel (green line), or both (blue line). (B) Immunoblot analyses for proteins indicated on the right using lysates prepared from PDX4 of mice that were not treated (Control) or treated with cirmtuzumab, paclitaxel, or both as indicated. The numbers below each row are the ratios of band densities as in Fig. 4E. (C) Table providing the numbers of mice that developed PDXs (numerator) versus the numbers of mice engrafted (denominator) with cells from either PDX4 or PDX5 (as indicated in the top row) that were removed from mice treated with hlgG, cirmtuzumab, paclitaxel, or cirmtuzumab and paclitaxel (as indicated in the far left column). The mice were given varying numbers of tumor cells as indicated in the row below the PDX designation. The *Bottom* provides a photograph of representative tumors that developed in mice engrafted with tumor cells from PDX4 of mice that were untreated or treated with cirmtuzumab and/or paclitaxel as indicated.

ROR1. Conversely, inhibiting BMI1 with a small molecule PTC-209 could enhance the sensitivity to chemotherapy and inhibit metastases in squamous cell carcinoma or inhibit the growth of colon cancer or breast cancer cells (12, 44).

The stemness of ROR1^{Hi} breast cancer cells, in part, also could be related to the activation of the Hippo-YAP/TAZ pathway. Prior studies found that Rho-GTPase activation could induce the Hippo-YAP/TAZ signaling, which could enhance the survival and self-renewal of human-embryonic stem cells (25). Moreover, coexpression of ROR1 with either FZD2 or FZD5 could induce dephosphorylation YAP and the accumulation of TAZ, leading to the activation of Hippo-YAP/TAZ signaling in HEK293A cells (26). Similarly, we found the expression of ROR1 was associated with the expression and nuclear localization of TAZ in primary breast cancer cells and that Wnt5a could enhance nuclear accumulation of TAZ in a ROR1-dependent manner. Furthermore, the expression of ROR1 also could promote EMT, which could enable epithelial breast cancer cells to migrate to distal sites (17).

The anti-ROR1 mAb cirmtuzumab may be effective in reversing cancer stemness. In a recently completed phase I trial involving patients with relapse/refractory CLL, treatment with cirmtuzumab inhibited leukemia-cell activation of Rho-GTPases and ROR1-signaling (14). Moreover, treatment with cirmtuzumab reversed the stemness gene expression signature of leukemia cells noted before therapy (14). This is similar to what we noted here in studies using mice engrafted with breast cancer PDXs; treatment with cirmtuzumab but not control hIgG repressed the expression of genes induced by the activation of Rho-GTPases, Hippo-YAP/TAZ, or BMI1. Moreover, cirmtuzumab also repressed the expression of genes that were up-regulated in EMT or CD44⁺/CD24^{Low} CSC. Such reprogramming was associated with impaired engraftment and reduced capacity to develop metastases in immune-deficient mice.

Agents that inhibit cancer stemness may complement the antitumor activity of chemotherapy by eliminating drug-resistant CSC or inhibiting the capacity of tumor cells to acquire features of CSCs. We found that treatment of either ER⁺ or ER⁻ breast cancer PDXs with paclitaxel and cirmtuzumab had significantly

greater antitumor activity than treatment with either agent alone. We speculate that cirmtuzumab or other agents that can inhibit ROR1 signaling may improve the response to chemotherapy and enhance the survival of patients with breast cancer.

Materials and Methods

Breast Cancer Specimens. We used anonymized archived formalin-fixed paraffin-embedded tumor tissues excised from patients ($n = 22$) with invasive ductal carcinoma before and after treatment with four to six cycles of docetaxel (T) at 75 mg/m² \pm doxorubicin (A) at 75 mg/m² or epirubicin (E) at 75 mg/m² \pm cyclophosphamide (C) at 600 mg/m² (docetaxel/epirubicin/doxorubicin, docetaxel/doxorubicin/cyclophosphamide, docetaxel/epirubicin, or epirubicin and cyclophosphamide) at Sun Yat-set University Cancer Center, China. Each patient had a core needle biopsy or excisional biopsy before neoadjuvant chemotherapy and had surgical resection of residual tumors after chemotherapy.

Primary breast tumor tissues used to generate PDXs were obtained from biopsy material of patients with breast adenocarcinoma after they provided written informed consent. Experiments involving these samples were approved by the Institutional Review Board of UC San Diego (HRPP090401) in accordance with the Declaration of Helsinki.

Spheroid Formation Assay. Some 300–10,000 viable single cells were plated on Ultra Low Attachment 6-well or 96-well plates (Corning Incorporated Life Sciences) and cultured in MEGMTM mammary epithelial cell growth medium (Lonza) with or without recombinant Wnt5a (R&D system) at 100 ng/mL for 1–3 wk. Spheroids with sizes greater than 100 μ m were counted using an inverted microscope (Nikon). A more detailed description of the reagents, biochemistry assays, cellular analysis, and animal studies are provided in *SI Appendix, Materials and Methods*.

ACKNOWLEDGMENTS. We thank Victoria Tripple for technical assistance in the PDX studies and Dennis Young for flow-cytometry analysis and sorting. We acknowledge the help of the Histology Core Laboratory for processing tissue specimens, Dr. Nissi Varki for histology and immunohistochemistry assessments, and the University of California San Diego Moores Cancer Center Biorepository and Tissue Technology Shared Resource for PDX samples. This paper was supported by the National Key Projects of Research and Development of China (Grant 2016YFC0904600), the National Natural Science Foundation of China (Grant 81672912), the Science and Technology Foundation of Shenzhen, China (Shenzhen Peacock Innovation Team Project, Grant KQTD20140630100658078), the Breast Cancer Research Foundation (Grant BCRF-17-120), National Institutes of Health Grant P01-CA081534, and the California Institute for Regenerative Medicine.

- Creighton CJ, et al. (2009) Residual breast cancers after conventional therapy display mesenchymal as well as tumor-initiating features. *Proc Natl Acad Sci USA* 106: 13820–13825.
- Kimbung S, et al.; PROMIX Trialists Group (2018) Assessment of early response biomarkers in relation to long-term survival in patients with HER2-negative breast cancer receiving neoadjuvant chemotherapy plus bevacizumab: Results from the Phase II PROMIX trial. *Int J Cancer* 142:618–628.
- Ye X, et al. (2015) Distinct EMT programs control normal mammary stem cells and tumour-initiating cells. *Nature* 525:256–260.
- Wahl GM, Spike BT (2017) Cell state plasticity, stem cells, EMT, and the generation of intra-tumoral heterogeneity. *NPJ Breast Cancer* 3:14.
- Battle E, Clevers H (2017) Cancer stem cells revisited. *Nat Med* 23:1124–1134.
- Arteaga CL (2013) Progress in breast cancer: Overview. *Clin Cancer Res* 19:6353–6359.
- Al-Hajj M, Wicha MS, Benito-Hernandez A, Morrison SJ, Clarke MF (2003) Prospective identification of tumorigenic breast cancer cells. *Proc Natl Acad Sci USA* 100: 3983–3988.
- Wang Y, et al. (2012) Cancer stem cell marker Bmi-1 expression is associated with basal-like phenotype and poor survival in breast cancer. *World J Surg* 36:1189–1194.
- Grinstein E, Mahotka C (2009) Stem cell divisions controlled by the proto-oncogene Bmi-1. *J Stem Cells* 4:141–146.
- Lukacs RU, Memarzadeh S, Wu H, Witte ON (2010) Bmi-1 is a crucial regulator of prostate stem cell self-renewal and malignant transformation. *Cell Stem Cell* 7: 682–693.
- Wu X, et al. (2011) Silencing of Bmi-1 gene by RNA interference enhances sensitivity to doxorubicin in breast cancer cells. *Indian J Exp Biol* 49:105–112.
- Kreso A, et al. (2014) Self-renewal as a therapeutic target in human colorectal cancer. *Nat Med* 20:29–36.
- Paranjape AN, et al. (2014) Bmi1 regulates self-renewal and epithelial to mesenchymal transition in breast cancer cells through Nanog. *BMC Cancer* 14:785.
- Choi MY, et al. (2018) Phase I trial: Cirmutuzumab inhibits ROR1 signaling and stemness signatures in patients with chronic lymphocytic leukemia. *Cell Stem Cell* 22:951–959.e3.
- Zhang S, et al. (2012) ROR1 is expressed in human breast cancer and associated with enhanced tumor-cell growth. *PLoS One* 7:e31127.
- Zhang S, et al. (2012) The onco-embryonic antigen ROR1 is expressed by a variety of human cancers. *Am J Pathol* 181:1903–1910.
- Cui B, et al. (2013) Targeting ROR1 inhibits epithelial-mesenchymal transition and metastasis. *Cancer Res* 73:3649–3660.
- Chien HP, et al. (2016) Expression of ROR1 has prognostic significance in triple negative breast cancer. *Virchows Arch* 468:589–595.
- Fukuda T, et al. (2008) Antisera induced by infusions of autologous Ad-CD154-leukemia B cells identify ROR1 as an oncofetal antigen and receptor for Wnt5a. *Proc Natl Acad Sci USA* 105:3047–3052.
- Pukrop T, et al. (2006) Wnt 5a signaling is critical for macrophage-induced invasion of breast cancer cell lines. *Proc Natl Acad Sci USA* 103:5454–5459.
- Iozzo RV, Eichstetter I, Danielson KG (1995) Aberrant expression of the growth factor Wnt-5A in human malignancy. *Cancer Res* 55:3495–3499.
- Yu J, et al. (2016) Wnt5a induces ROR1/ROR2 heterooligomerization to enhance leukemia chemotaxis and proliferation. *J Clin Invest* 126:585–598.
- Fritz G, Just I, Kaina B (1999) Rho GTPases are over-expressed in human tumors. *Int J Cancer* 81:682–687.
- Hein AL, et al. (2016) RAC1 GTPase promotes the survival of breast cancer cells in response to hyper-fractionated radiation treatment. *Oncogene* 35:6319–6329.
- Ohgushi M, Minaguchi M, Sasai Y (2015) Rho-signaling-directed YAP/TAZ activity underlies the long-term survival and expansion of human embryonic stem cells. *Cell Stem Cell* 17:448–461.
- Park HW, et al. (2015) Alternative Wnt signaling activates YAP/TAZ. *Cell* 162:780–794.
- Cordenonsi M, et al. (2011) The Hippo transducer TAZ confers cancer stem cell-related traits on breast cancer cells. *Cell* 147:759–772.
- Bartucci M, et al. (2015) TAZ is required for metastatic activity and chemoresistance of breast cancer stem cells. *Oncogene* 34:681–690.
- Moroishi T, Hansen CG, Guan KL (2015) The emerging roles of YAP and TAZ in cancer. *Nat Rev Cancer* 15:73–79.
- Ginestier C, et al. (2007) ALDH1 is a marker of normal and malignant human mammary stem cells and a predictor of poor clinical outcome. *Cell Stem Cell* 1:555–567.
- Samanta D, Gilkes DM, Chaturvedi P, Xiang L, Semenza GL (2014) Hypoxia-inducible factors are required for chemotherapy resistance of breast cancer stem cells. *Proc Natl Acad Sci USA* 111:E5429–E5438.
- Schaefer CF, et al. (2009) PID: The pathway interaction database. *Nucleic Acids Res* 37: D674–D679.
- Liberzon A, et al. (2011) Molecular signatures database (MSigDB) 3.0. *Bioinformatics* 27:1739–1740.
- Li C, et al. (2017) A ROR1-HER3-lncRNA signalling axis modulates the Hippo-YAP pathway to regulate bone metastasis. *Nat Cell Biol* 19:106–119.
- Wiederschain D, et al. (2007) Contribution of polycomb homologues Bmi-1 and Mel-18 to medulloblastoma pathogenesis. *Mol Cell Biol* 27:4968–4979.
- Taube JH, et al. (2010) Core epithelial-to-mesenchymal transition interactome gene-expression signature is associated with claudin-low and metaplastic breast cancer subtypes. *Proc Natl Acad Sci USA* 107:15449–15454.
- Ben-Porath I, et al. (2008) An embryonic stem cell-like gene expression signature in poorly differentiated aggressive human tumors. *Nat Genet* 40:499–507.
- Kim J, Hwangbo J, Wong PK (2011) p38 MAPK-mediated Bmi-1 down-regulation and defective proliferation in ATM-deficient neural stem cells can be restored by Akt activation. *PLoS One* 6:e16615.
- Desai N, et al. (2006) Increased antitumor activity, intratumor paclitaxel concentrations, and endothelial cell transport of cremophor-free, albumin-bound paclitaxel, ABI-007, compared with cremophor-based paclitaxel. *Clin Cancer Res* 12:1317–1324.
- Gilbert LA, Hemann MT (2010) DNA damage-mediated induction of a chemoresistant niche. *Cell* 143:355–366.
- Milanovic M, et al. (2018) Senescence-associated reprogramming promotes cancer stemness. *Nature* 553:96–100.
- McHenry PR, Vargo-Gogola T (2010) Pleiotropic functions of Rho GTPase signaling: A Trojan horse or Achilles' heel for breast cancer treatment? *Curr Drug Targets* 11: 1043–1058.
- Nacerddine K, et al. (2012) Akt-mediated phosphorylation of Bmi1 modulates its oncogenic potential, E3 ligase activity, and DNA damage repair activity in mouse prostate cancer. *J Clin Invest* 122:1920–1932.
- Srinivasan M, et al. (2017) Downregulation of Bmi1 in breast cancer stem cells suppresses tumor growth and proliferation. *Oncotarget* 8:38731–38742.